Nucleic Acids Research, 1993, Vol. 21, No. 24 5547–5553

Stability of triple helices containing RNA and DNA strands: experimental and molecular modeling studies

Christophe Escudé, Jean-Christophe François, Jian-sheng Sun*, Günther Ott[1], Mathias Sprinzl[1], Thérèse Garestier and Claude Hélène

Laboratoire de Biophysique, Muséum National d'Histoire Naturelle, INSERM U201, CNRS UA481, 43 rue Cuvier 75005 Paris, France and [1]Laboratorium für Biochemie, Universität Bayreuth, Postfach 10 12 51, 8580 Bayreuth, Germany

Received October 22, 1993; Accepted November 5, 1993

ABSTRACT

UV-absorption spectrophotometry and molecular modeling have been used to study the influence of the chemical nature of sugars (ribose or deoxyribose) on triple helix stability. For the Pyrimidine.Purine* Pyrimidine motif, all eight combinations were tested with each of the three strands composed of either DNA or RNA. The chemical nature of sugars has a dramatic influence on triple helix stability. For each double helix composition, a more stable triple helix was formed when the third strand was RNA rather than DNA. No stable triple helix was detected when the polypurine sequence was made of RNA with a third strand made of DNA. Energy minimization studies using the JUMNA program suggested that interactions between the 2'-hydroxyl group of the third strand and the phosphates of the polypurine strand play an important role in determining the relative stabilities of triple-helical structures in which the polypyrimidine third strand is oriented parallel to the polypurine sequence. These interactions are not allowed when the third strand adopts an antiparallel orientation with respect to the target polypurine sequence, as observed when the third strand contains G and A or G and T/U. We show by footprinting and gel retardation experiments that an oligoribonucleotide containing G and A or G and U fails to bind double helical DNA, while the corresponding DNA oligomers form stable triple-helical complexes.

INTRODUCTION

Triple helices were first observed in 1957 for homo-polyribonucleotides (1), then for polydeoxyribonucleotides and hybrids (2,3). More recently, the binding of short oligonucleotides to oligopyrimidine-oligopurine sequences of double-helical DNA has been described (4–6). These oligonucleotides are developed to control gene expression at the transcriptional level in the so-called 'antigene strategy' (see ref. 7 for a review) and to modify and/or cleave long DNA fragments at single sites (see ref. 8 for a review). A pyrimidine oligonucleotide binds to the major groove of a double helix in a parallel orientation with respect to the purine strand, through formation of Hoogsteen hydrogen bonds between a T.A base pair and thymine and between a C.G base pair and protonated cytosine (4–7). Oligonucleotides containing G and A (9,10) or G and T (11,12) can also be involved as a third strand to form a triple helix.

Triple helix-forming oligonucleotides can compete with the binding of transcription factors (13–15) and affect transcription initiation (15–17) or elongation (18,19). A triple helix approach can also be used to target a single-stranded nucleic acid, using either a linear oligonucleotide forming both Watson–Crick and Hoogsteen hydrogen bonds (20,21) or a circular oligonucleotide (22,23). A more specific recognition and a higher affinity for the targets are thus obtained. An RNA oligonucleotide can also bind to a DNA double helix (24,25). Other duplexes such as double-helical RNA, RNA hairpins or DNA-RNA hybrids are involved in biological processes and could be substrates for oligonucleotide binding.

Here, we report the results of an experimental and molecular modeling study of the influence of sugar composition (ribose or deoxyribose) on the stability of Py.Pu*Py and Py.Pu*Pu triple helices. In the notation X.Y*Z, the '.' represents Watson–Crick pairing between the oligopyrimidine strand (strand I) and the oligopurine strand (strand II) of the double helix, while the '*' represents Hoogsteen pairing between strand II and the third strand which is either parallel (oligopyrimidine) or antiparallel (oligopurine) to strand II. Triple helix stability was measured by absorption spectroscopy or by footprinting and gel retardation methods. Determination of energy minimized structures provides information regarding interstrand interactions. While this work was in progress, reports by Roberts and Crothers (26) and Han and Dervan (27) also addressed the same question of triple helix stability for different combinations of RNA and DNA strands for the Py.Pu*Py motif. Another study recently compared the ability of RNA and DNA oligonucleotides to repress bacteriophage promoters (28).

* To whom correspondence should be addressed

MATERIALS AND METHODS

23-mer R1 and R2 oligoribonucleotide synthesis

Two 23-mer oligoribonucleotides were synthesized by the H-phosphonate method. 2'-O-(t-butyldimethylsilyl)-5'-O-(4,4'-dimethoxytrityl)-uridine-3'-H-phosphonate and 2'-O-(t-butyldimethylsilyl)-5'-O-(4,4'-dimethoxytrityl)-N^4-benzoyl-cytidine-3'-H-phosphonate were synthesized according to known procedures (29). N^6-dimethylaminomethylene-protected 2'-O-(t-butyldimethylsilyl)-5'-O-(4,4'-dimethoxytrityl)-adenosine and N^2-dimethylaminomethylene-protected 2'-O-(t-butyldimethyl-silyl)-5'-O-(4,4'-dimethoxytrityl)-guanosine were prepared according to Arnold *et al.* (30) and converted to the 3'-H-phosphonates by a slightly modified method of Froehler *et al.* (31). CPG-supports with spacer and the start-up nucleosides (25−40 mmol/g) were prepared as described (30).

Automated RNA synthesis was performed on a Gene Assembler Plus DNA-synthesizer from Pharmacia. 1-adamantanecarbonyl chloride and tetrabutylammonium fluoride were purchased from Fluka. Dichloroacetic acid in dichloroethane came from Pharmacia, low-water-containing pyridine and acetonitrile were from Baker. The H-phosphonates were dissolved in pyridine/acetonitrile (1/1) to a concentration of 0.12 M each. 1-adamantanecarbonyl chloride was dissolved in the same solution to reach a concentration of 0.48 M. Automated oligoribonucleotide synthesis was performed according to a modified synthesizer program, as compared to the synthesis of DNA. The coupling time for each cycle was elevated from 1 min for DNA synthesis to 2 min for RNA synthesis. Coupling was achieved by 5 successive pulses (1.2 seconds) each of 0.12 M H-phosphonate and 0.48 M 1-adamantanecarbonyl chloride solution to the CPG column (flow rate 2.5 ml/min), coated with 1.5 mmol start-up nucleoside. Then the activated H-phosphonates were recycled through the column for 2 min.

At the end of the synthesis, the oxidation of the polymer-bound oligomeric H-phosphonates was achieved by a two-step procedure according to Froehler *et al.* (31). Cleavage of the crude oligonucleotide from the CPG support and deprotection of the bases was performed in a one-step procedure by treatment of the CPG support with ethanol/25 % ammonia (1/3; v/v) for 48 hrs at room temperature. After filtration, the resulting solution was evaporated to dryness. The remaining 2'-blocked oligoribonucleotide was dissolved in 0.9 ml of 1M tetrabutylammonium fluoride in DMF (N,N-dimethylformamide) and incubated at room temperature for 24 hrs. The resulting crude RNA was desalted and analysed by 20 % PAGE in the presence of 7 M urea. The average coupling efficiencies were about 98 % and the synthesis amounts were 138 A_{260} (45 %, based on 1.5 mmol start-up nucleoside) in the case of CCUGAUAAA-GGAGGAGAUGAAGA and 144 A_{260} (48 %, based on 1.5 mmol start-up nucleoside) in the case of UCUUC-AUCUCCUCCUUUAUCAGG.

Other oligonucleotides

All other oligonucleotides were obtained from Eurogentec (Seraing, Belgium). The two 23-mer DNA strands were suspended in bidistilled water, gel-filtered on a Sephadex Quick Spin G25 column and then precipitated with 5 volumes of ethanol in the presence of 0.3 M sodium acetate, and washed with ethanol. The pellet was lyophilized and resuspended in bidistilled water.

The oligoribonucleotides were 2'-O-protected with Fpmp = [1-(2-fluorophenyl)-4-methoxy-piperidin-1-yl] groups. They were deprotected by adding 600 ml of 0.01 M sterile aqueous HCl to the desalted, purified oligomer. The solution was incubated for 20 hours at 20°C, then neutralized with 15 ml of 2.0 M Tris HCl pH 8.3. The protecting groups were removed by filtering the solution on a NAP 10 column (Pharmacia) with 5 ml elution buffer (11-mer) or by precipitating with 1-butanol (23- and 27-mer).

Concentrations of oligonucleotides were estimated by UV absorption, using sequence-dependent absorption coefficients given by a nearest-neighbor model (32).

UV absorption

Thermal denaturation profiles were obtained with a Kontron Uvikon 820 or 940 spectrophotometer, using 1 cm optical path length quartz cuvettes. The cell holder was thermostated by a circulating liquid (80% water / 20% ethyleneglycol). The temperature of one of the cuvettes was measured via thermoresistance. The temperature in the water bath was increased or decreased at a rate of 0.1°C/mn, thus allowing complete thermal equilibrium of the cells between two measurements. Reading of absorbance at 260 nm and 540 nm was performed every 10 minutes. The absorbance at 540 nm (used as a reference for the stability of the spectrophotometer) was substracted from that at 260 nm. The concentration of the duplex was 1 μM, while that of the third strand was 1.2 μM. The temperature was first decreased from 80°C to 0°C and then raised from 0°C to 80°C .

Gel retardation assay

A non-denaturing 10% acrylamide gel (99:1 acrylamide/bis-acrylamide) containing 20 mM Hepes buffer, pH 7.2, and 20 mM $MgCl_2$ was prepared. The homopyrimidine strand of the duplex was labeled by T4 polynucleotide kinase using [γ-^{32}P]ATP, precipitated and resuspended in water. Various concentrations of the third strand were added to 10 nM of duplex. The mixture was preincubated at 37°C for one night in a pH 7.2, 50 mM Hepes buffer containing 20 mM $MgCl_2$, 100 mM NaCl, 10% sucrose, 0.5 μg/μl tRNA and 0.1 mM spermine. Electrophoresis was then performed for 2 hours at 37°C.

Footprinting studies

Footprinting studies were carried out using DNase I as a cleaving reagent. Radiolabeled duplex was incubated in the presence of either the triple helix-forming oligonucleotide (DNA or RNA) or a nonspecific oligonucleotide. For (C,T/U)-containing oligonucleotides, we used a phosphate buffer (50 mM, pH 6) containing 0.1 M NaCl, 0.5 mM spermine and 5 mM $MgCl_2$. For (G,A)- or (G,T/U)-containing oligonucleotides, the buffer was Hepes (50 mM, pH 7.2) with 0.5 mM spermine, 0.1 M NaCl and 10 mM $MgCl_2$. DNase I was added and the reaction was stopped 10 s later by ethanol precipitation.

Molecular modeling

Conformational energy minimization was performed with the JUMNA program (version VII) which is specifically designed for modeling nucleic acids (33). The net charge of each phosphate group was set to −0.5 charge unit, equally shared by the two adjacent ionized oxygens, to mimic counter-ion screening effects. No water molecules were explicitly taken into account in this calculation. Their effect was simulated by the use of a sigmoidal

distance-dependent dielectric function. Triple helices were built from a library of ribo- and deoxyribonucleotides by specifying helicoidal parameters in agreement with the Cambridge convention. Starting points corresponded to the triple helix model obtained from fiber diffraction data (34) or other structures obtained in earlier studies (35,36). The cytosines belonging to strand III were protonated in order to give rise to two Hoogsteen hydrogen bonds with guanines in strand II. Some parameters (helical parameters, sugar pucker, etc.) were constrained to adopt a specific range of values. Various conformations for the sugar pucker (C3'-endo or N-type, C2'-endo or S-type) were investigated for each strand. A wide range of conformations was scanned in order to obtain the best energy-minimized structure. In each case, the investigated triplexes were 10 base triplets in length. Different triple helices were studied: $T_{10}.A_{10}*T_{10}$ (where T is replaced by U when the nucleotide is a ribonucleotide) and $C_{10}.G_{10}*C+_{10}$ for the parallel motif and $C_{10}.G_{10}*G_{10}$ for the antiparallel motif. Constraints were imposed so that a base triplet was the repetitive unit in the triple-helical structure. These computations were performed on a Silicon Graphics 4D/420 GTXB workstation. Molecules were visualized with the help of the Insight II software (BIOSYM) fully interfaced with the JUMNA program.

RESULTS

Thermal dissociation of Py.Pu*Py triple helices measured by UV absorption spectroscopy

The four different 23 bp duplexes that could be made with the oligonucleotides R1, R2, D1, and D2 (figure 1) were used as substrates for oligonucleotide binding. These duplexes contain an 11 bp oligopyrimidine-oligopurine sequence which is a target for binding of either the RNA (R3) or DNA (D3) 11 mer oligopyrimidine. This oligopyrimidine-oligopurine sequence was previously studied as substrate for the binding of β- and α-oligodeoxyribonucleotides and oligonucleotide-intercalator conjugates (37,38). The double helix was chosen to be longer (23 base pairs) than the triple-helical complex (11 base triplets) so that its melting occurs at much higher temperature than the triplex-to-duplex transition. Thermal dissociation experiments were carried out at pH 6.0 in a cacodylate buffer (10 mM) containing 100 mM NaCl, 0.1 mM EDTA and 1 mM spermine (figure 2). Under these conditions, half-dissociation of the D3 oligopyrimidine from the D1.D2 double helix occurred at 32°C while the duplex melted at a much higher temperature (66°C). Under the same conditions, we could detect transitions from triplex to duplex + single strand for only six out of the eight possible triplexes. For the mixtures R1.R2*D3 and D1.R2*D3, only the transition corresponding to the melting of the duplex was observed. Slow kinetics of formation and dissociation were observed for three triple helices, R1.D2*D3, D1.R2*R3 and R1.R2*R3, which did not exhibit a reversible melting profile (figure 2). This hysteresis phenomenon was previously described in detail for a triple helix containing 22 base-triplets (39). In the absence of spermine, all melting profiles exhibited hysteresis at a rate of heating (cooling) of 0.1°C/mn. The presence of an RNA

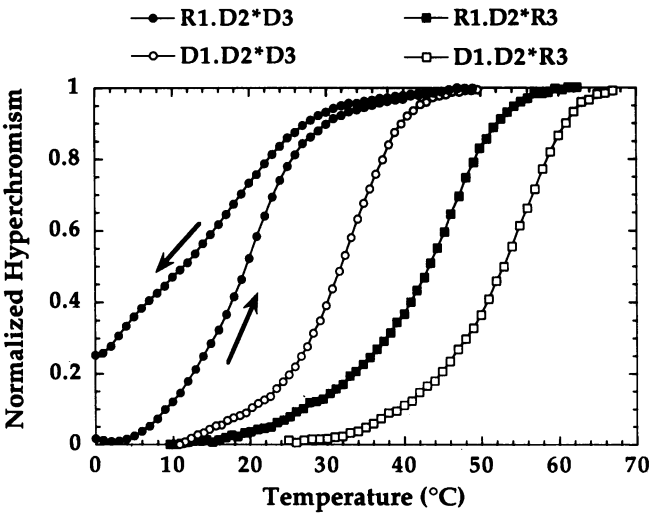

Figure 2. Denaturation profiles for the mixture of 11-mer oligonucleotide (1.2 μM) R3 (squares) and D3 (circles) with the 23 bp-long duplex (1 μM) D1.D2 (open symbols) and R1.D2 (closed symbols) in a pH 6 cacodylate buffer (10 mM) containing 0.1 M NaCl and 1 mM spermine. Absorbance of the duplex was substracted from that of the mixture of duplex and third strand and the hyperchromism due to triplex dissociation was then normalized. No hyperchromism could be observed for the D1.R2*D3 and R1.R2*D3 combinations. Upon decreasing and increasing the temperature at a rate of 0.1°C/min, the profiles for R1.D2*D3 were not superimposable. Arrows indicate the direction of the temperature variation. The same phenomenon was observed with the D1.R2*R3 and R1.R2*R3 combinations (profiles not shown). All other profiles were reversible.

```
                5' CCTGAT AAAGGAGGAGA TGAAGA 3'
                3' GGACTA TTTCCTCCTCT ACTTCT 5'

D1          3' d(GGACTATTTCCTCCTCTACTTCT) 5'
R1          3' r(GGACUAUUUCCUCCUCUACUUCU) 5'
D2          5' d(CCTGATAAAGGAGGAGATGAAGA) 3'
R2          5' r(CCUGAUAAAGGAGGAGAUGAAGA) 3'
D3                5' d(TTTCCTCCTCT) 3'
R3                5' r(UUUCCUCCUCU) 3'
```

Figure 1. Sequences of the various DNA and RNA oligonucleotides (D1, R1, D2, R2, D3, R3) used to investigate the stability of the eight combinations of strands in triple-helical complexes (see table I). The target sequence for triplex formation is boxed on the duplex DNA (D1.D2) shown at the top.

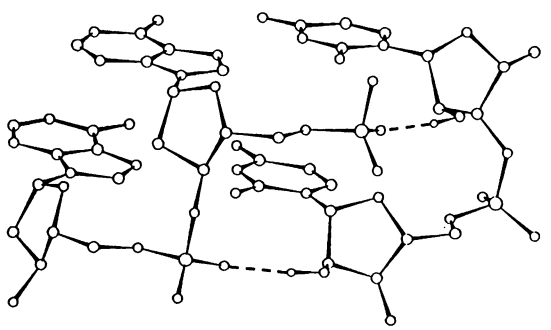

Figure 3. Model extracted from the energy-minimized structure of a dT.dA*rU triple helix containing 10 base triplets. It illustrates the possibility of hydrogen bonding interaction between the hydroxyl group of a ribose in strand III and one of the oxygen atoms belonging to the phosphate group in strand II (dashed line). For sake of clarity, only two nucleotides of strands II and III have been drawn, and hydrogen atoms are not shown except those from the 2'-hydroxyl groups.

Table I. Half dissociation temperatures (T_m) for triple helices studied in a 10mM cacodylate buffer (pH 6) in the presence of 0.1M NaCl and 1mM spermine.

I.II.III	T_m(°C)
D1.D2*D3	32
D1.D2*R3	54
D1.R2*D3	N.O.
D1.R2*R3	16*
R1.D2*D3	13*
R1.D2*R3	43
R1.R2*D3	N.O.
R1.R2*R3	11*

Strands I and II correspond to the Watson–Crick double helix with the oligopyrimidine sequence on strand I and the oligopurine sequence on strand II. Strand III is the Hoogsteen hydrogen-bonded third strand. N.O. indicates that no transition could be attributed to the formation of a triple helix. Asterisks indicate that the kinetics of the reaction are slow; the dissociation curves were obtained after maintaining the sample for 8 hours at 0°C, then heating at a rate of 0.1°C/mn, and the indicated half-dissociation temperatures (T_m) are the average between apparent T_m values obtained from association and dissociation curves.

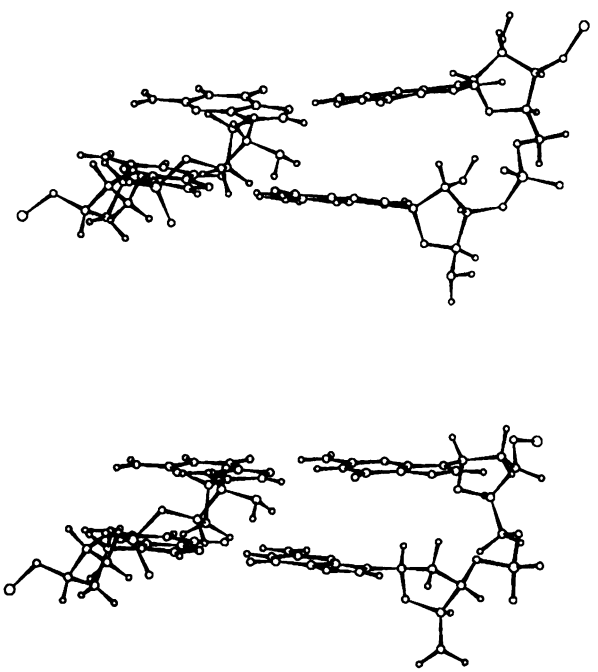

Figure 4. Model extracted from the energy minimized structures of dC.dG*rG (top) and dC.dG*dG (bottom) triple helices to illustrate the position of the hydroxyl group in a Reverse Hoogsteen configuration. For sake of clarity, only two nucleotides of strands II and III have been drawn.

strand in the triple helix is generally characterized by slower kinetic rates, in particular for the association step. For non-reversible profiles, the dissociation curves wee obtained after maintaining the sample for 8 hours at 0°C, and then heating at a rate of 0.1°C/mn. The half-dissociation temperatures (T_m) given in table I are the average between apparent values obtained from association and dissociation curves. The comparison of the half-dissociation temperatures for the triplex-to-duplex transition indicates a dramatic influence of the nature of sugar moieties in each strand on the stability of the triplex (table I). As observed previously for triple helices formed with oligodeoxynucleotides, decreasing the pH increased the stability of the triple helices

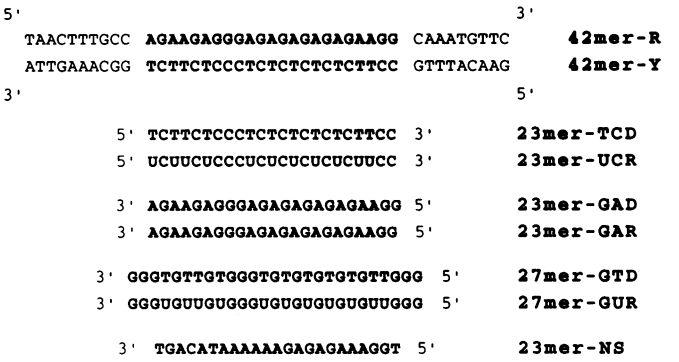

Figure 5. Sequences of the various DNA and RNA oligonucleotides used for gel retardation and footprinting experiments.

containing oligoribonucleotides. At pH 5.5, the relative stability of triple helices was similar to that at pH 6 (results not shown). The most stable triple helix was found to be D.D*R followed by R.D*R, then D.D*D, while the three less stable complexes, whose formation was very slow, were found to have stabilities decreasing in the order D.R*R = R.D*D = R.R*R.

Molecular modeling

In order to understand the difference in stability observed when changing the third strand from DNA to RNA, we investigated the structure of triple helices obtained after energy minimization using the JUMNA program. Our energy-minimized models suggest that, for the Py.Pu*Py motif, the 2'-OH groups of the third strand interact favorably with the phosphate groups of strand II (figure 3). The distance between the hydroxyl group and one of the oxygen atom of the phosphate is 1.93 Å.

For the Py.Pu*Pu motif, the hydroxyl groups on the third strand point toward the neighboring sugar on the 5'-side of the same strand and are sterically unfavorable in the triple-helical structure (figure 4). NMR studies of an intramolecular triple helix involving C.G*G and T.A*T base triplets showed that the 2',2'-hydrogen atoms of the third strand were pointing toward the next base on the 5'-side of the same strand (40). This position resulted in large upfield shifts of the 2',2' protons. Replacement of the 2'-proton by a 2'-hydroxyl leads to a distortion of the third strand conformation. These molecular modeling studies suggested that an RNA third strand should be less favored than a DNA third strand when reverse Hoogsteen hydrogen bonding interactions are involved in triple helix formation, as observed with third strands containing G and A or G and T/U which bind in an antiparallel orientation with respect to the purine-containing strand II (9–12). This is in contrast to what was predicted for the parallel Py.Pu*Py motif where an RNA third strand is favored compared to a DNA third strand, as experimentally observed (see above). We tested this conclusion by comparing the relative stability of triple helices formed upon binding of (C, T/U)-, (G,A)- and (G,T/U)-containing oligonucleotides to a DNA double helix. The results which are presented below are in agreement with the above predictions.

Comparative studies of Py.Pu*Py and Py.Pu*Pu triple helices

Gel retardation. The stability of Py.Pu*Py triple helices was investigated by absorption spectroscopy. Triple helix formation in the Py.Pu*Pu motif is more difficult to analyze by

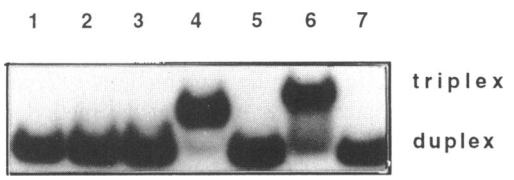

Figure 6. Gel retardation experiments at pH 7.2 and 37°C in a buffer containing 50 mM phosphate, 20 mM $MgCl_2$ and 0.2 mM spermine. Lane 1: control duplex (42 bp, see figure 5). Lane 2: 50 μM (C,T)-DNA (23mer-TCD). Lane 3: 50 μM (C,U)-RNA (23mer-UCR). Lane 4: 20 μM (G,A)-DNA (23mer-AGD). Lane 5: 50 μM (G,A)-RNA (23mer-AGR). Lane 6: 20 μM (G,T)-DNA (27mer-GTD). Lane 7: 50 μM (G,U)-RNA (27mer-GUR).

spectroscopic experiments because G-containing oligonucleotides often self-associate and the hyperchromic effects associated with the triplex-to-duplex transition are smaller. Therefore, gel retardation experiments were carried out to compare the binding of RNA and DNA third strands to double-helical DNA. A longer triple helix was necessary to visualize triple helix formation by gel retardation. The sequences of the oligonucleotides used in these experiments are described on figure 5. First, we compared the affinity of a DNA (23TC) and an RNA (23UC) third strand for binding to the 42 bp target sequence. In polyacrylamide gels, the mobility of the triple helix was retarded relative to the corresponding duplex, as shown in previous publications (11,18). It was possible to quantitate the amount of double and triple helix in presence of various concentrations of third strands. Apparent association constants (K_a) were determined to be 1.6×10^7 M^{-1} for 23UC and 2×10^6 M^{-1} for 23TC at 37°C in a pH 6 phosphate buffer (50mM) containing 0.1 M NaCl, 0.2 mM spermine and 5 mM $MgCl_2$ (results not shown). Footprinting experiments (see below) also showed that 23UC was bound more strongly than 23TC to its double-helical target. Thus, these results confirm the spectroscopic results obtained with the 11 bp target sequence described above. A higher stability was observed when an RNA instead of a DNA third strand binds to double-helical DNA in the Py.Pu*Py motif.

We then compared the ability of (G,A)- or (G,T)-containing oligodeoxynucleotides and (G,A) or (G,U)-containing oligoribonucleotides to bind a DNA double-helix (figure 6). The binding of (G,A)- and (G,T/U)-containing oligonucleotides is not pH-dependent. Therefore, the study was carried out at pH 7.2. At 37C, the (C,T/U)-containing oligonucleotides did not form a stable triple helix at pH 7.2 in the buffer used for the purine-containing oligonucleotides. This is in agreement with melting temperatures measurements. In the presence of 0.1M NaCl, 1mM spermine and 5mM $MgCl_2$, the T_m of the (C,T)-23mer decreased from 29 to 23°C when pH increased from 6 to 7.2. For the (C,U)-23mer, the corresponding values were 34 and 30°C. Therefore, at pH 7.2 and 37°C it was unlikely to detect a triple helix by gel retardation. In contrast, (G,A)- and (G,T)-containing DNA third strands formed stable triple helices. Under the conditions described in figure 6, the apparent association constants were estimated to be 2×10^6 M^{-1} and 10^5 M^{-1} for (G,A)- and (G,T)-containing oligodeoxynucleotides, respectively. In contrast, neither (G,A)-, nor (G,U)-containing oligoribonucleotides formed triple helices stable enough to be detected by gel retardation, even at a 50 μM concentration of third strand (figure 6). It should be kept in mind that the orientation of (G,T/U)-containing oligonucleotides depends on

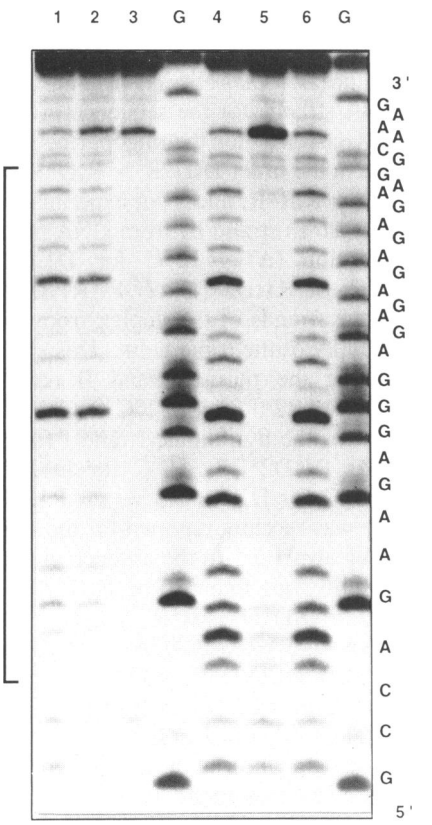

Figure 7. DNase I footprinting experiments carried out at pH 6.0 (lanes 1–3) or at pH 7.2 (lanes 4–6). Lanes 1 and 4 are controls using the 42 bp DNA fragment shown on figure 5. Lane 2: in the presence of 1 μM (T,C)-DNA (23mer-TCD). Lane 3: in the presence of 1 mM (U,C)-RNA (23mer-UCR). Lane 5: in the presence of 20 μM (G,A)-DNA (23mer-GAD). Lane 6: in the presence of 20 μM (G,A)-RNA (23mer-GAR). Lanes indicated 'G' are Maxam–Gilbert sequencing lanes for guanines. The vertical bar on the left indicates the triple helix site. The polypurine-containing strand of the 42 bp DNA fragment was 5'-end labelled. Note that even though there is no footprint observed for the (C,T)-DNA at 1 μM (lane 2), this footprint was clearly observed when the concentration was raised to 10 μM (not shown).

the sequence, especially on the number of GpT and TpG steps (12). The sequence used in the present study strongly favors an antiparallel orientation with respect to the polypurine target sequence. Both the (G,T/U)- and (G,A)-containing oligonucleotides were synthesized to bind in such an antiparallel orientation.

Footprinting experiments. Footprinting experiments confirmed the results obtained by gel retardation studies (figure 7). Binding of an oligonucleotide to double-helical DNA inhibits DNAse I strand cleavage. The results clearly show that an oligoribonucleotide binds more strongly than an oligodeoxynucleotide in the Py.Pu*Py motif at pH 6. At pH 7.2, an oligoribonucleotide containing G and A gave no footprint whereas an oligodeoxynucleotide protected the target from strand cleavage. Similar results were obtained with (G,T)-DNA as compared to (G,U)-RNA: a footprint was obtained with the oligodeoxunucleotide but not with its ribose-containing analogue. The (G,A)-DNA was bound more strongly than the (G,T)-DNA as determined by the concentration dependence of the footprints (results not shown). These results are in agreement with the gel retardation experiments described above.

DISCUSSION

The relative stabilities of triple helices containing all combinations of DNA and RNA strands for the sequence investigated here, i.e., $^{5'}$AAAGGAGGAGA$^{3'}$ for the oligopurine sequence, were found to decrease in the order D.D*R > R.D*R > D.D*D > D.R*R = R.D*D = R.R*R, under our experimental conditions. Changing the Hoogsteen strand III from DNA to RNA induced a strong stabilization (ΔT_m=22°C for D1.D2*R3 *versus* D1.D2*D3, 30°C for R1.D2*R3 *versus* R1.D2*D3). In our study, changing the strands of the duplex from DNA to RNA decreased the stability of the triple helix. This effect was much more important for the purine strand II (ΔT_m=38°C for D1.D2*R3 *versus* D1.R2*R3 and 32°C for R1.D2*R3 *versus* R1.R2*R3), than for the pyrimidine strand I (ΔT_m=19°C for D1.D2*D3 *versus* R1.D2*D3, 11°C for D1.D2*R3 *versus* R1.D2*R3, and 5°C for D1.R2*R3 *versus* R1.R2*R3).

A similar study was recently reported for the sequence $^{5'}$GGAGAGGAGGGA$^{3'}$ at pH 5.5 in the absence of spermine (26). The order of stability was found to be R.D*R > D.D*R > R.R*R > R.D*D > D.D*D, D.R*R. A more recent study with the sequence $^{5'}$AAAAGAAAAAAGAAAAGA$^{3'}$ reported the following order: D.D*D, D.D*R, R.D*R, R.D*D > D.R*R, R.R*R (27). The difference in stability between the different triple helices was much less important in the second case than in the first one. Our results are closer to those reported by Roberts and Crothers. These differences might reflect differences in base sequences and in experimental conditions (pH, salts). The three studies conclude that a DNA purine strand II stabilizes the triple helix. Our study, like that of Roberts and Crothers, concludes that an RNA third strand stabilizes triple helices as compared to a DNA third strand (see also references 24,25), whereas that of Han and Dervan does not reveal any important effect. The relative stabilities of the complexes are very different in the three reported cases. In all studies, the combinations R.R*D and D.R*D were found to be very unstable and were not detected either by UV spectroscopy or by quantitative affinity cleavage titration. Double-helical nucleic acids with an oligopurine RNA sequence on strand II appear to exclude DNA as a third strand, at least for such short sequences.

Changing a DNA into an RNA strand results in the loss of a methyl group from T and in the addition of the 2'-hydroxyl group which induces a preferred N-type sugar pucker but may also be involved in direct or water-mediated intrastrand and interstrand interactions (41). Recently, hydrogen bonds between 2'-hydroxyl and 5'-oxygen or phosphate oxygen atoms, have been inferred from X-ray crystallography data in double-helical DNA-RNA duplexes, in addition to the previously observed hydrogen bonds to 1'-oxygens of adjacent nucleotides (42). Our model suggests a possible direct hydrogen bond between the 2'OH groups of strand III and the phosphate groups of strand II in the Py.Pu*Py motif where the third strand binds parallel to the polypurine strand II via Hoogsteen hydrogen bonding. Such interactions cannot take place when a strand III containing G and A or G and U binds to a double helix in a reverse Hoogsteen hydrogen-bonding configuration. Footprinting and gel retardation experiments with 23-mer oligoribonucleotides have shown that an RNA strand III containing G and A or G and U binds much more weakly to a DNA double-helix than its DNA counterpart.

Triple helices have been shown to be stabilized when strand III is synthesized 2'-O-methyl derivatives (24–25). Methyl substitution of the 2'-OH groups in strand III obviously prevents hydrogen bonding interactions with phosphate groups of strand II. Molecular modeling studies and energy minimization suggest that the loss of hydrogen bonding interactions is compensated by Van der Waals interactions involving the methyl groups.

Skoog and Maher (28) compared the ability of DNA or RNA oligonucleotides to repress transcription by site-specific triple helix formation. For the Py.Pu*Py motif, they found that DNA oligonucleotides provide a slightly smaller inhibition than RNA oligonucleotides. For the Py.Pu*Pu motif, they did not observe any effect of oligoribonucleotides, in agreement with our footprinting and gel retardation experiments.

The influence of the nature of the sugars in the duplex strands on triple helix stability is more difficult to interpret. Recent experiments have shown that the sugar pucker of the purine strand in Py.Pu*Py triple-helices adopts a C2'-endo conformation (43–46). Replacing a DNA purine strand II by an RNA changes the sugar pucker into a C3'-endo conformation. This conformation might be unfavorable to triplex formation. Strand II interacts with both strands I and III and might have to be flexible enough to optimize these interactions.

The influence of several parameters on the stability of triple helices containing RNA strands remains to be explored. In these interactions, hydrophobic effects may also play an important role. They have been suggested to be involved in triple helix stabilization involving three DNA strands. Methyl groups at the C-5 position of cytosines in strand III stabilize triple helices, probably because these methyl groups together with those of thymine form a 'spine' of hydrophobic interactions which contributes to triple helix stability (47). The effect of methyl group substitution at the 5-position of uracil and cytosine in a triple helix-forming oligoribonucleotide remains to be explored. The synthesis of such oligoribonucleotides is under way. Deformations have been shown to take place at the junctions between a double-helix and a triple helix (48). When RNA strands are present in a triple-helix, these deformations might be different. Polycations, such as spermine, may interact differently with RNA- and DNA-containing triple helices. Their effect on the kinetics of triple helix formation might also depend on the RNA/DNA composition of the three strands.

The results presented here show that the structure of the canonical Py.Pu*Py triple helix exhibits an important polymorphism, influenced by the sequence and the chemical nature of the sugars, as does the double helix itself. In these structures, interactions between strand II and strand III are favored when strand III is an RNA.

When the third strand contains G and A, it binds in an antiparallel orientation with respect to the Watson–Crick oligopurine sequence (9,10). This holds true also for third strands containing G and T (11) even though the orientation may depend on the distribution of G's and T's in the oligonucleotide (12). Changing the orientation of the third strand changes the interactions that its sugars may engage with the Watson-Crick strands. Therefore the properties of Py.Pu*Py triple helices do not apply when the third strand contains G and A or G and T/U. Results comparing the binding of several oligonucleotides to a 23 bp oligopurine.oligopyrimidine sequence of double-helical DNA indicate that a (C,U)-containing oligoribonucleotide binds more strongly than a (C,T)-containing oligodeoxynucleotide, as observed for other sequences. In contrast, a (G,A)- and a (G,U)-containing RNA do not bind to a double-helical DNA target under conditions where a (G,A)- and a (G,T)-containing DNA bind to this sequence. These and forthcoming studies should provide a

rational basis to synthesize the more appropriate oligonucleotide that provides the highest triplex stability and specificity when targeting a DNA duplex, an RNA duplex or an RNA-DNA double-helical hybrid. These results should also be taken into account when designing oligonucleotide clamps (20,21) and circular oligonucleotides (22,23) which form triple-helical complexes when they bind to single stranded nucleic acids. Chimeric DNA-RNA oligonucleotides should be considered for such applications.

ACKNOWLEDGEMENTS

This work was supported by grants from the Association Nationale de Recherche sur le SIDA (ANRS) and from Rhône-Poulenc Rorer. The work of Christophe Escudé was supported by a financial grant from IFSBM.

REFERENCES

1. Felsenfeld, G., Davies, D.R. & Rich A. (1957) *J. Am. Chem. Soc.*. **79**, 2023.
2. Riley, M., Maling, B. and Chamberlin, M.J. (1966) *J. Mol. Biol.* **20**, 359–389.
3. Morgan, A.R. and Wells, R.D. (1968) *J. Mol. Biol.* **37**, 63.
4. Le Doan T., Perrouault L., Praseuth D., Habhoub N., Decout J.L., Thuong N.T., Lhomme J. & Hélène C. (1987) *Nucl. Acids Res.* **15**, 7749–7760.
5. Moser H.E. & Dervan P.B. (1987) *Science* **238**, 645–650.
6. Lyamichev, V.I., Mirkin, S.M., Frank-Kamenetskii, D. and Cantor, C.R. (1988) *Nucl. Acids Res.* **16**, 2165–2178.
7. Hélène C. (1991) *Anti-Cancer Drug Design* **6**, 569–584.
8. Hélène C. (1993) *Current Opinion in Biotechnology* **4**, 29–36.
9. Beal, P.A. and Dervan, P.B. (1991) *Science* **251**, 1360–1363.
10. Pilch, D.S., Levenson, C. and Shafer, R.H. (1991) *Biochemistry* **30**, 6081–6087.
11. Durland, R.H., Kessler, D.J., Gunnell, S., Duvic, M., Pettitt, B.M. and Hogan, M.E. (1991) *Biochemistry* **30**, 9246–9255.
12. Sun, J.S., De Bizemont, T., Duval-Valentin, G., Montenay-Garestier, T. and Hélène, C. (1991) *C. R. Acad. Sci. Paris*, Série III, **313**, 585–590.
13. Postel, E.H., Flint, S.J., Kessler, D.J. and Hogan, M.F. (1991) *Proc. Natl. Acad. Sci.* **88**, 8227–8231.
14. Grigoriev, M., Praseuth, D., Robin, P., Hemar, A., Saison-Behmoaras, T., Dautry-Varsat, A., Thuong, N.T., Hélène, C. and Harel-Bellan, A. (1992) *J. Biol. Chem.* **267**, 3389–3395.
15. Maher, L.J., Wold, B. and Dervan, P.B. (1989) *Science* **245**, 725.
16. Maher, L.J., III (1992) *Biochemistry* **31**, 7587–7594.
17. Grigoriev, M., Praseuth, D., Guyesse, A.L., Robin, P., Thuong, N.T., Hélène, C. and Harel-Bellan, A. (1993) *C. R. Acad. Sci., Life sciences* **316**, 492–495.
18. Young, S.L., Krawczyk, S.H., Matteucci, M.D. and Toole, J.J. (1991) *Proc. Natl. Acad. Sci.* **88**, 10023–10026.
19. Duval-Valentin, G., Thuong, N.T. and Hélène, C. (1992) *Proc. Natl. Acad. Sci. U.S.A.* **89**, 504–508.
20. Giovannangeli, C., Montenay-Garestier, T., Rougée, M., Chassignol, M., Thuong, N.T., and Hélène, C. (1991) *J. Am. Chem. Soc.* **113**, 7775- 7777.
21. Giovannangeli, C., Thuong, N.T. and Hélène, C. (1993) *Proc. Natl. Acad. Sci. U.S.A.* in the press.
22. Kool, E.T. (1991) *J. Am. Chem. Soc.* **113**, 6265–6266.
23. Prakash, G. and Kool, E.T. (1992) *J. Am. Chem. Soc.* **114**, 3523–3527.
24. Shimizu, M., Konishi, A., Shimada, Y., Inoue, H. and Ohtsuka, E. (1992) *FEBS Letters*, **302**, 155–158.
25. Escudé, C., Sun, J.S., Rougée, M., Garestier, T. and Hélène, C. (1992) *C. R. Acad. Sci. Paris*, Série III, **315**, 521–525.
26. Roberts, R.W. and Crothers, D.M. (1992) *Science* **258**, 1463–1466.
27. Han, H. and Dervan, P.B. (1993) *Proc. Natl. Acad. Sci. U.S.A.* **90**, 3806–3810.
28. Skoog, J.U. and Maher III, L.J. (1993) *Nucl. Acids Res.* **21**, 2131–2138.
29. Stawinski, J., Strömberg, R., Thelin, M. and Westman, E. (1988) *Nucl. Acids Res.* **16**, 9285–9298.
30. Arnold, L., Smrt, J., Zajicek, J., Ott, G., Schiesswohl, M. and Sprinzl, M. (1991) *Collect. Czech. Chem. Commun.* **56**, 1948–1956.
31. Froehler, B.C., Ng, P.G. and Matteucci, M.D. (1986) *Nucl. Acids Res.* **14**, 5399–5407.
32. Cantor, C.R. and Warshaw, M.M. (1970) *Biopolymers* **9**, 1059–1077.
33. Lavery, R. (1988) in *Structure and expression Vol. 3 DNA bending and curvature*, (Olson, W.K., Sarma, M.H., Sarma, R.H. and Sundaralingam, M., Eds) Adenine Press, 191–211.
34. Arnott S. & Selsing E. (1974) *J. Mol. Biol.* **88**, 509–521.
35. Liquier, J., Coffinier, P., Firon, M. and Taillandier, E. (1991) *J. Biomol. Struct. Dyn.* **9**, 437–445.
36. Akhebat, A., Dagneaux, C., Liquier, J., and Taillandier, E. (1992) *J. Biomol. Struct. Dyn.* **10**, 577–588.
37. Sun, J.S., François, J.C., Montenay-Garestier, T., Saison-Behmoaras, T., Roig, V., Chassignol, M., Thuong, N.T. and Hélène, C. (1989) *Proc. Natl. Acad. Sci. U.S.A.* **86**, 9198–9202.
38. Sun, J.S., Giovannangeli, C., François, J.C., Kurfurst, R., Montenay-Garestier, T., Asseline, U., Saison-Behmoaras, T., Thuong, N.T. and Hélène, C. (1989) *Proc. Natl. Acad. Sci. U.S.A.* **88**, 6023–3027.
39. Rougée, M., Faucon, B., Mergny, J.L., Barcelo, F., Giovannangeli, C., Garestier, T. and Hélène, C. (1992) *Biochemistry* **31**, 9269–9278.
40. Radhakrishnan, I. and Patel, D.J. (1993) *J. Am. Chem. Soc.* **115**, 1615–1617.
41. Saenger, W. (1984) in: Principles of Nucleic Acid Structure (Cantor, C.R. ed.) Springer Verlag, New-York.
42. Egli, M., Usman, N. and Rich, A. (1993) *Biochemistry* **32**, 3221–3237.
43. Howard, F.B., Todd Miles, H., Keliang liu, Frazier, J., Raghunathan, G. and Sasisekharan, V. (1992) *Biochemistry* **31**, 10671–10677.
44. Ouali, M., Letellier, R., Adnet, F., Liquier, J., Sun, J.S., Lavery, R. and Taillandier, E. (1993) *Biochemistry* , **32**, 2098–2103.
45. Macaya, R.F., Schultze, P. and Feigon, J. (1992) *J. Am. Chem. Soc.* **114**, 781.
46. Macaya, R.F., Wang, E., Schultze, P. and Feigon, J. (1992) *J. Mol. Biol.* **225**, 755.
47. Sun, J.S. and Hélène, C. (1993) *Current Opinion in structural biology* , **3**, 345–356.
48. Chomilier, J., Sun, J.S., Collier, D.A., Garestier, T., Hélène C. and Lavery, R. (1992) *Biophysical Chemistry* **45**, 143–152.